Physica B 405 (2010) 3685–3689

Contents lists available at ScienceDirect

Physica B

journal homepage: www.elsevier.com/locate/physb

Up-conversion fluorescence and thermal optical bistability in Gd_2O_3: 10% Yb^{3+}, 0.5% Tm^{3+}

Chunyan Cao [a,*], Xianmin Zhang [b], Minglun Chen [a], Weiping Qin [c], Jisen Zhang [d]

[a] College of Mathematics and Physics, Jinggangshan University, Ji'an 343009, PR China
[b] Department of Physics, Liaoning University, Shenyang 110036, PR China
[c] State Key Laboratory on Integrated Optoelectronics, College of Electronic Science and Engineering, Jilin University, Changchun 130012, PR China
[d] Key Laboratory of Excited State Processes, Changchun Institute of Optics, Fine Mechanics and Physics, Chinese Academy of Sciences, Changchun 130033, PR China

ARTICLE INFO

Article history:
Received 25 April 2010
Received in revised form
20 May 2010
Accepted 21 May 2010

Keywords:
Gd_2O_3: 0.5% Tm^{3+}
10% Yb^{3+}
Phase
Excitation power
Up-conversion fluorescence
Thermal optical bistability

ABSTRACT

Through a co-precipitation method $Gd(OH)_3$: 0.5% Tm^{3+}, 10% Yb^{3+} powder was synthesized. After sintering at different temperatures, the as-prepared $Gd(OH)_3$: 0.5% Tm^{3+}, 10% Yb^{3+} powder was changed into cubic and monoclinic phase Gd_2O_3: 0.5% Tm^{3+}, 10% Yb^{3+} phosphors. Crystalline phases and morphologies of as-prepared powder and phosphors were characterized by X-ray diffraction (XRD) and field emission scanning electron microscope (FE-SEM). Up-conversion (UC) fluorescence spectra of Gd_2O_3: 0.5% Tm^{3+}, 10% Yb^{3+} phosphors were recorded by a fluorescence spectrophotometer with a 980 nm continuous wave laser diode as the excitation source. Fluorescence decay behaviors of the phosphors were measured by exciting with 980 nm from an optical parametric oscillator (OPO) pumped by a pulsed Nd: YAG laser with a pulse duration of 10 ns and a repetition frequency of 10 Hz, and the signal was recorded using a monochromator and an oscillograph. Phase and excitation power dependent UC fluorescence properties of the phosphors were studied in detail in the article. Interestingly, the cubic phase phosphors presented thermal optical bistability phenomena. The fluorescence dynamic analysis indicated that rise and decay processes existed in the phosphor UC fluorescence.

1. Introduction

Rare earth sesquioxides (RE_2O_3) are well known to crystallize in various structures according to the radius of RE ions. Gadolinium oxide (Gd_2O_3) crystallized in a cubic C-type structure (space group $Ia\bar{3}$) and was changed into monoclinic B-type structure (space group C2/m) at higher temperatures [1]. The cubic phase Gd_2O_3 can also appear at a very high temperature (2200 °C) from the hexagonal phase Gd_2O_3 [2]. On the other hand, lowering symmetry sites in host matrix would cause an increase in transition probability of activators, resulting in stronger fluorescence intensities. For example, Patra et al.[3] and Patra [4] had studied optical properties of RE ions in different phase host matrices and found that lower symmetric structures would result in longer excited state lifetimes and higher fluorescence intensities of phosphors [3,4].

Gd_2O_3 is a well-known material used not only in monocrystal and powder states but also in thin-film forms. As reported in the literature, Gd_2O_3 is selected as host material for optical studies employing Eu^{3+}, Er^{3+}, Nd^{3+}, and Tm^{3+} ions as dopants due to its good chemical, photo-thermal, and photo-chemical stabilities, and its low phonon-energy [5–13]. Frequency up-conversion (UC) is widely studied in RE-doped materials for RE ion's ample levels and monochromatic fluorescence in visible and ultraviolet (UV) optical regions. For RE-doped Gd_2O_3, UC fluorescence studies were mainly focused on the cubic phase Gd_2O_3 with only a few considering on the monoclinic phase Gd_2O_3 [9,14,15].

In this paper $Gd(OH)_3$: 0.5% Tm^{3+}, 10% Yb^{3+} powder was synthesized through a co-precipitation method. After calcining at different temperatures in air, the as-prepared $Gd(OH)_3$: 0.5% Tm^{3+}, 10% Yb^{3+} powder was changed into different phase Gd_2O_3: 0.5% Tm^{3+}, 10% Yb^{3+} phosphors. The phosphors emitted bright blue UC fluorescence under 980 nm laser diode excitation. Blue UC fluorescent properties of the phosphor's dependence on phases and excitation powers as well as fluorescent dynamics were studied.

2. Experimental

The Gd_2O_3: 0.5% Tm^{3+}, 10% Yb^{3+} phosphors were prepared by a combinational method of co-precipitation and calcination procedures. In the preparation, 20 mmol stoichiometric amounts

* Corresponding author. Tel.: +86 796 8100489; fax: +86 796 8124959.
E-mail address: caoyan_80@126.com (C. Cao).

0921-4526/$ - see front matter © 2010 Elsevier B.V. All rights reserved.
doi:10.1016/j.physb.2010.05.066

of Gd_2O_3, Tm_2O_3, and Yb_2O_3 were dissolved in hydrochloric acid (HCl) at an elevated temperature to form a clear solution; at the same time 144 mmol NaOH was dissolved in distilled water. Then the NaOH solution was added dropwise into the hydrochloric solution to form $Gd(OH)_3$ suspension solution under vigorous stirring. After washing with deionized water for more than three times, the resultant material was dried at 60 °C for 10 h in vacuum condition and as-prepared $Gd(OH)_3$: 0.5% Tm^{3+}, 10% Yb^{3+} powder was obtained. After sintering at 900, 1000, 1200, 1300, and 1400 °C for 2 h in air, the as-prepared powder was changed into different phase Gd_2O_3: 0.5% Tm^{3+}, 10% Yb^{3+} phosphors.

Crystalline phases, sizes, and morphologies of as-prepared powder and phosphors were characterized by powder X-ray diffraction (XRD); (Model Rigaku RU-200b) using nickel-filtered CuKα target radiation ($\lambda = 1.5406$ Å) and field emission scanning electron microscopy (FE-SEM) (Hitachi S-4800), respectively. In the UC fluorescence experiment, a semiconductor of 980 nm continuous wave laser diode with a maximum power of 2 W was used to pump the phosphors. UC fluorescence spectra of phosphors were recorded using a Hitachi fluorescence spectrophotometer (F-4500). Fluorescence decay curves of phosphors were measured by exciting with 980 nm from an optical parametric oscillator (OPO) pumped by a pulsed Nd: YAG laser with a pulse duration of 10 ns and a repetition frequency of 10 Hz. The signal was recorded using a monochromator and an oscillograph. All of the measurements were performed at room temperature.

3. Results and discussion

3.1. Characterization

Fig. 1 illustrates the XRD patterns of as-prepared and sintered powders at 900, 1000, 1200, 1300, and 1400 °C for 2 h $Gd(OH)_3$: 0.5% Tm^{3+}, 10% Yb^{3+}. According to JCPDS standard cards, the as-prepared $Gd(OH)_3$ powder exhibited hexagonal structure. After sintering at relatively low temperatures (900, 1000, and 1200 °C), the $Gd(OH)_3$ powder was changed into cubic phase Gd_2O_3 phosphors. From the narrowed peaks of patterns we learnt that the crystallite sizes increased with the increase of calcined temperatures. After calcined at 1300 °C, the Gd_2O_3 phosphor exhibited mixed cubic and monoclinic phases, but the cubic phase predominated over the monoclinic. After calcined at 1400 °C for 2 h, the $Gd(OH)_3$ powder was entirely changed into monoclinic Gd_2O_3. As evident in the XRD patterns, the $Gd(OH)_3$ was changed into cubic phase Gd_2O_3 below 1300 °C and was entirely changed into the monoclinic phase Gd_2O_3 at 1400 °C. It is well-known that the monoclinic phase material is less symmetric than the cubic phase material. These results clearly indicated the dependence of crystal structures and symmetries on sintering temperatures.

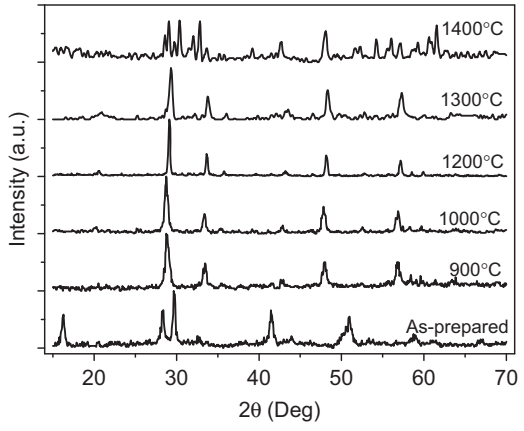

Fig. 1. XRD patterns of $Gd(OH)_3$: 0.5% Tm^{3+}, 10% Yb^{3+} as-prepared and sintered at different temperatures for 2 h , respectively.

Fig. 2 shows the corresponding FE-SEM images of samples. The as-prepared $Gd(OH)_3$: 0.5% Tm^{3+}, 10% Yb^{3+} powder has a nanorod-like morphology with an average diameter of 20–30 nm and length of 200–300 nm. After sintering at 900 and 1000 °C (Fig. 2(b), (c)) for 2 h, the nanorods changed little and only a small amount of them transformed into particles. However, there were major changes in morphology after the as-prepared powder was sintered at 1200 °C (Fig. 2(d)): the nanorod transformed into interlinked particles. The particles aggregated and grew further after sintering at 1300 °C and changed into bulk material after sintering at 1400 °C. Crystallite sizes and morphologies changed greatly with sintering temperatures, indicating that the annealing process not only changed phases but also affected sizes and morphologies of phosphors.

3.2. UC fluorescence spectra

UC fluorescence spectra of Gd_2O_3: 0.5% Tm^{3+}, 10% Yb^{3+} phosphors sintered at 1300 and 1400 °C in the wavelength range of 400–510 nm are shown in Fig. 3(a) and (b), respectively. Both spectra were obtained under the same measurement conditions (e.g. Em slit = 1.0 nm, high voltage of photomultiplier tube (PMT) = 700 V, excitation power = 600 mW, etc.). A weak shoulder corresponding to the $^1D_2 \rightarrow {}^3F_4$ transition appeared at about 453 nm, and the fluorescence in the wavelength range 456–510 nm was assigned to the $^1G_4 \rightarrow {}^3H_6$ transition [7,16]. There were some differences in UC fluorescence spectra of the phosphors sintered at two temperatures. In the cubic phase phosphor (sintered at 1300 °C), the emission $^1G_4 \rightarrow {}^3H_6$ had two distinct peaks at about 475 and 486 nm (the energy difference was 477 cm^{-1}), which corresponds well with Refs. 7,11. In the monoclinic phase phosphor (sintered at 1400 °C), the $^1G_4 \rightarrow {}^3H_6$ transition had only one main peak at about 475 nm. The fluorescent spectra indicated that the crystalline phases of the phosphors had great effects on the spectral profiles and the emission peak positions. Concrete for these reasons will be discussed in the following text.

Fig. 4 shows UC fluorescence spectra of the two phosphors under different excitation powers. Fig. 4(a) and (b) shows UC spectra of cubic (sintered at 1300 °C) and monoclinic (sintered at 1400 °C) phase Gd_2O_3: 0.5% Tm^{3+}, 10% Yb^{3+} phosphors, respectively. From the bottom up in both of the sub-figures, the excitation powers were 200, 250, 350, and 600 mW. With increase of excitation powers, the spectra has different variation trends besides increase in intensities. For the cubic phase phosphor, at lower excitation power the emission peaking at 475 nm was weaker than the peak at 486 nm, while at higher excitation power the emission peak at 475 nm became the main emission and occupied about 70% intensity of the $^1G_4 \rightarrow {}^3H_6$ transition, which inclined to the spectral shape of the monoclinic phase phosphor. For the monoclinic phase phosphor, the fluorescence intensities became stronger monotonously with increase of excitation powers.

To understand phase (sintering temperatures) and excitation powder dependent UC fluorescence spectra clearly, we plotted UC florescent spectra of cubic (sintered at 1300 °C) and monoclinic (sintered at 1300 °C) phase phosphors under different excitation powers in Fig. 5. As shown in this figure, solid line and dashed line are the UC spectra of cubic and monoclinic phase Gd_2O_3: 0.5% Tm^{3+}, 10% Yb^{3+} phosphors, respectively, which were all normalized to the emission peak at 475 nm. Under lower

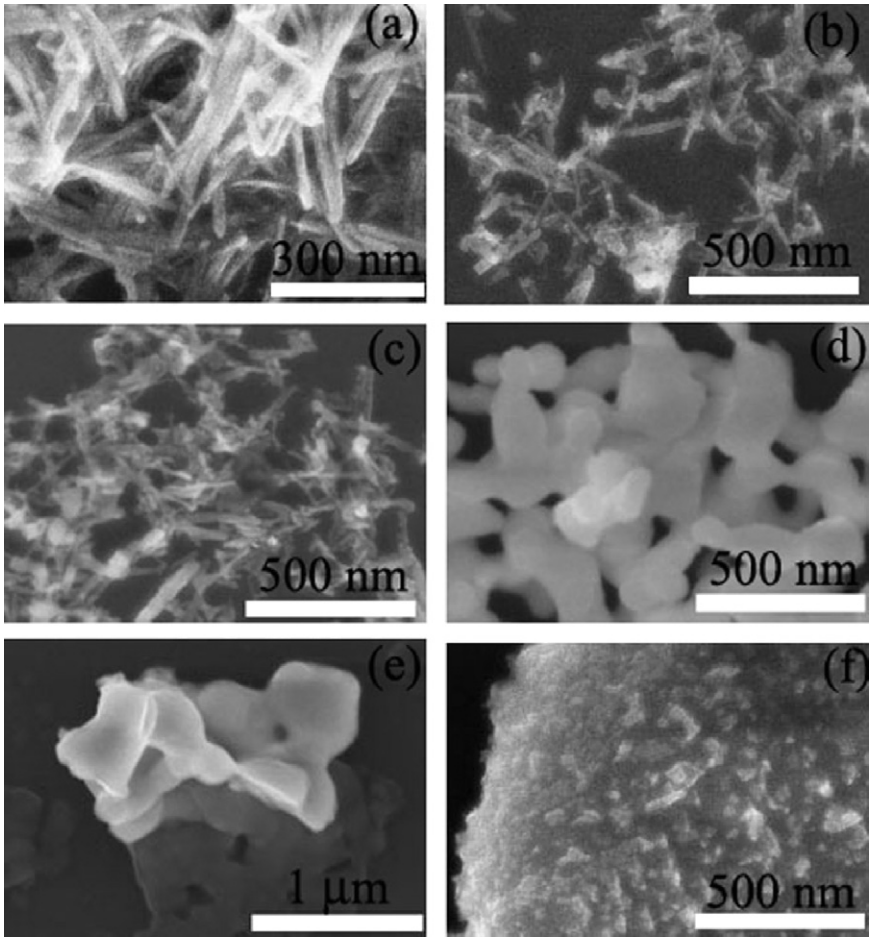

Fig. 2. SEM images of $Gd(OH)_3$: 0.5% Tm^{3+}, 10% Yb^{3+} (a) as-prepared, sintered at (b) 900, (c) 1000, (d) 1200, (e) 1300, and (f) 1400 °C for 2 h.

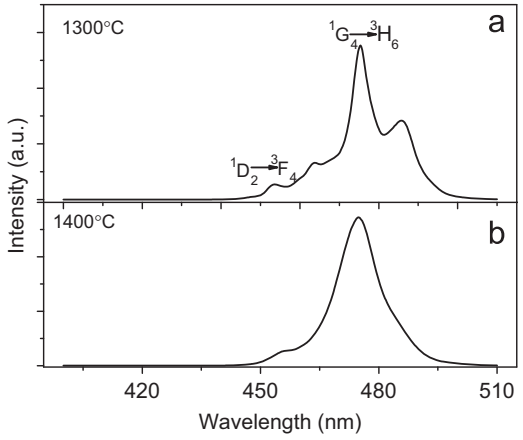

Fig. 3. Up-conversion fluorescence spectra of Gd_2O_3: 0.5% Tm^{3+}, 10% Yb^{3+}: (a) cubic and (b) monoclinic phase .

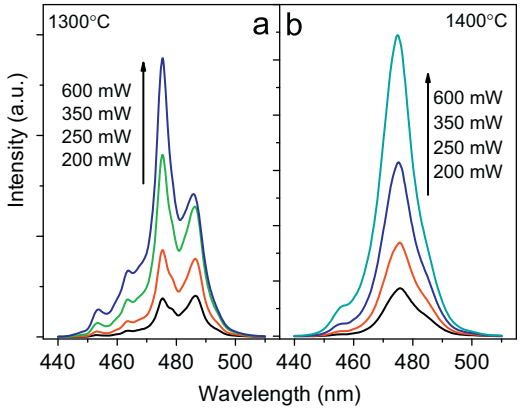

Fig. 4. Excitation power dependent up-conversion fluorescence spectra of Gd_2O_3: 0.5% Tm^{3+}, 10% Yb^{3+}: (a) cubic and (b) monoclinic phase .

excitation power the UC fluorescence of cubic phosphor concentrated on the 486 nm fluorescence, while at higher excitation power the UC fluorescence peak at about 475 nm predominated over that at 486 nm, which had trends similar to those of the monoclinic phase phosphor.

As shown in Fig. 3, the sintering process had great effects on the profiles of UC fluorescence spectra of the two phosphors. However, the phosphors sintered at 900, 1000, 1200, and 1300 °C had similar spectral profiles and variation trends as shown in Fig. 6. Fig. 6 (a) and (b) presents UC fluorescent spectra of the above cubic phase phosphors excited under 150 and 600 mW, respectively. Relative intensities of the two peaks changing with excitation powers are common in cubic phase phosphors. In fact, UC fluorescent intensities become stronger with increase in the of sintered temperatures under the same measurement conditions.

In addition, cubic phase phosphors presented thermal optical bistability phenomena. In phosphors, the local thermal effect caused by laser irradiation was evident under high excitation powers [17], which led to the temperature-dependent optical bistability. The variation of relative intensities of 475 and 486 nm

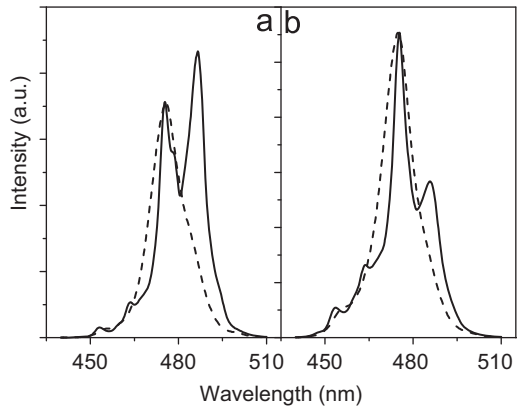

Fig. 5. Up-conversion fluorescence spectra of cubic (solid line) and monoclinic (dashed line) phase Gd_2O_3: 0.5% Tm^{3+}, 10% Yb^{3+} with excitation powers (a) 150 mW and (b) 600 mW.

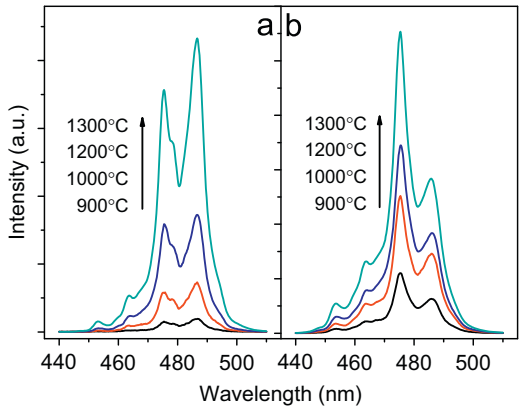

Fig. 6. Sintering temperature dependent up-conversion fluorescence spectra of Gd_2O_3: 0.5% Tm^{3+}, 10% Yb^{3+} with excitation powers (a) 150 mW and (b) 600 mW.

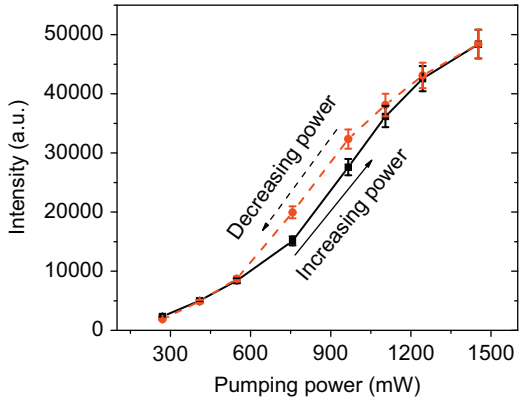

Fig. 7. Excitation power dependent up-conversion fluorescence of cubic phase Gd_2O_3: 0.5% Tm^{3+}, 10% Yb^{3+}.

emissions might be related to the thermal effect. Fig. 7 shows blue integrated fluorescence intensities as a function of excitation powers in the cubic phase Gd_2O_3: 0.5% Tm^{3+}, 10% Yb^{3+} phosphor (sintered at 1300 °C). The down-trace (black solid line through solid squares) show blue integrated fluorescence intensities as excitation powers gradually increase, while the up-trace (red dashed line through solid circles) display integrated intensities as excitation powers gradually decrease. In the down-trace, fluorescence intensities of the phosphor increase slowly initially and quickly and then slowly with increase in the excitation powers. In the up-trace, fluorescence intensities decreased in another way with decrease in the excitation powers. Distinct hysteresis loop was thereby formed. Similar hysteresis loops were observed in the other cubic phase phosphors. The fluorescence displayed a bistability phenomenon, which was possibly caused by non-radiative anharmonic phonon processes [18–20]. However, it is different from the intrinsic bistability phenomenon as described in the previous reference, which was dominated by nonlinear emission processes caused by coupling of Yb^{3+}–Yb^{3+} pairs [21].

From the UC fluorescence spectra shown above, we learn that not only phases (sintering temperatures) but also excitation powers have great effects on profiles and intensities of the spectra. To understand the UC fluorescence properties of the phosphors well, we studied fluorescence dynamic behaviors of the phosphors.

3.3. Fluorescence dynamics properties

The dynamics decay curve of UC fluorescence of Tm^{3+} in the monoclinic phase Gd_2O_3: 0.5% Tm^{3+}, 10% Yb^{3+} phosphor is shown in Fig. 8. As presented in the figure, the dynamic curve contains a fast rise process and a slow decay process. The rise process corresponds to the energy-transfer-induced population increase as the laser pulse was terminated originally, which depends strongly on energy transfer (ET) rate. Though the fluorescent dynamic curve had rise and decay profile, it could not be well fitted with a universal function $I(t)=I_0\exp(-t/\tau_2)-I_0\exp(-t/\tau_1)$, where τ_1 and τ_2 were rise and decay time constants, respectively. In the case,τ_1 depended mainly on the ET rate from Yb^{3+} to Tm^{3+} and τ_2 depended on the electronic transition rate of the related excited level. Other phosphors exhibited similar fluorescence dynamics behaviors.

To understand the UC fluorescence properties well, we resorted to the schematic energy-level diagrams of Yb^{3+} and Tm^{3+} ions as well as ET processes as shown in Fig. 9. Yb^{3+} ions were pumped to the $^2F_{5/2}$ level by absorbing 980 nm photons and the Tm^{3+} ions were excited to the $^1G_4$ level through three step ETs [22]: (1) a Tm^{3+} ion was excited to the $^3H_5$ level by the ET process: $^3H_6$ (Tm^{3+})+$^2F_{5/2}$ (Yb^{3+})→$^3H_5$ (Tm^{3+})+$^2F_{7/2}$ (Yb^{3+}), then this Tm^{3+} ion relaxes to the $^3F_4$ level; (2) the same Tm^{3+} ion was further excited to the $^3F_2$ ($^3F_3$) level by another ET process: $^3F_4$ (Tm^{3+})+$^2F_{5/2}$ (Yb^{3+})→$^3F_2$ ($^3F_3$) (Tm^{3+})+$^2F_{7/2}$ (Yb^{3+}) and then relaxed to the lower metastable $^3H_4$ state; and (3) a third excited Yb^{3+} ion transferred its excitation energy to this Tm^{3+} ion to excite it to the $^1G_4$ state: $^3H_4$ (Tm^{3+})+$^2F_{5/2}$ (Yb^{3+})→$^1G_4$ (Tm^{3+})+$^2F_{7/2}$ (Yb^{3+}). The left hand diagram corresponds to the longer wavelength emission and the right hand diagram consists

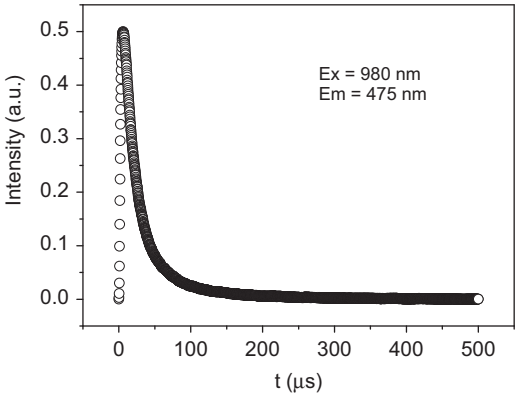

Fig. 8. Fluorescence dynamic curve for 475 nm emission in monoclinic phase Gd_2O_3: 0.5% Tm^{3+}, 10% Yb^{3+}.

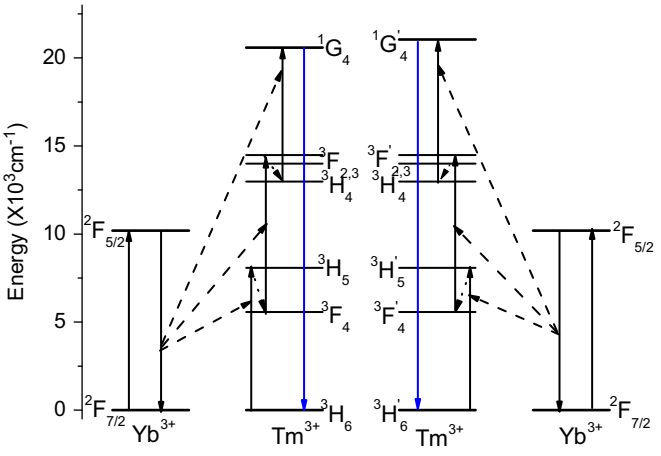

Fig. 9. Schematic energy level diagram illustrating mechanisms of Yb^{3+}-sensitized Tm^{3+} up-conversion fluorescence in Gd_2O_3 phosphors.

of the shorter wavelength emission. When the Tm^{3+} ions are located at different phase matrices, the energy levels would split slightly differently and result in different fluorescence spectral profiles of phosphors.

4. Conclusions

In conclusion, the as-prepared $Gd(OH)_3$: 0.5% Tm^{3+}, 10% Yb^{3+} powder was synthesized through a co-precipitation method. After sintering at different temperatures the powder was changed into cubic and monoclinic phase Gd_2O_3: 0.5% Tm^{3+}, 10% Yb^{3+} phosphors. Under 980 nm excitation, the phosphors exhibited bright blue UC fluorescence. Phase and excitation power dependent blue UC fluorescence properties of the phosphors were studied in detail in the article. The cubic phase phosphors exhibited thermal optical bistability phenomena. Fluorescence dynamic analysis indicated that rise and decay processes exist in the blue UC fluorescence of the Gd_2O_3: 0.5% Tm^{3+}, 10% phosphors.

Acknowledgements

This work was financially supported by the Natural Science Foundation of Jiangxi Province (Grant nos. 2009GQW0010, 2009GZW0012), the Science and Technology Program of Department of Education of Jiangxi Province (Grant no. GJJ10203), the National Natural Science Foundation of China (Grant nos. 10847141, 10774142, and 10874058), and the Research Program of Liaoning Educational Department (2009A308).

References

[1] S. Stecura, Research Report No. 6616, US Bureau of Mines, Washington, DC, 1964.
[2] J. Coutures, A. Rouanet, R. Verges, M. Foex, J. Solid State Chem. 17 (1976) 171.
[3] A. Patra, C.S. Friend, R. Kapoor, P.N. Prasad, Appl. Phys. Lett. 83 (2003) 284.
[4] A. Patra, Chem. Phys. Lett. 387 (2004) 35.
[5] A. Brenier, G. Boulon, J. Lumin. 82 (1999) 285.
[6] L.D. Sun, J. Yao, C.G. Liu, C.S. Liao, C.H. Yan, J. Lumin. 87–89 (2000) 447.
[7] H. Guo, N. Dong, M. Yin, W.P. Zhang, L.R. Lou, S.D. Xia, J. Phys. Chem. B 108 (2004) 19205.
[8] H. Guo, Y.F. Li, D.Y. Wang, W.P. Zhang, M. Yin, L.R. Lou, S.D. Xia, J. Alloys. Compd. 376 (2004) 23.
[9] T. Hirai, T. Orikoshi, J. Colloid Interface Sci. 269 (2004) 103.
[10] D. Dosev, I.M. Kennedy, M. Godlewski, I. Gryczynski, K. Tomsia, E.M. Goldys, Appl. Phys. Lett. 88 (2006) 11906.
[11] G. Jia, H.P. You, K. Liu, Y.H. Zheng, N. Guo, H.J. Zhang, Langmuir 26 (2010) 5122.
[12] J. Yang, C.X. Li, Z.Y. Cheng, X.M. Zhang, Z.W. Quan, C.M. Zhang, J. Lin, J. Phys. Chem. C 111 (2007) 18148.
[13] X.Y. Chen, E. Ma, G.K. Liu, M. Yin, J. Phys. Chem. C 111 (2007) 9638.
[14] A. Brenier, Chem. Phys. Lett. 290 (1998) 329.
[15] S.J. Yue, F. Wei, Y. Wang, Z.M. Yang, H.L. Tu, J. Du, J. Rare Earths 26 (2008) 371.
[16] G.S. Qin, W.P. Qin, C.F. Wu, S.H. Huang, D. Zhao, J.S. Zhang, S.Z. Lu, Opt. Commun. 242 (2004) 215.
[17] Y.Q. Lei, H.W. Song, L.M. Yang, L.X. Yu, Z.X. Liu, G.H. Pan, X. Bai, L.B. Fan, J. Chem. Phys. 123 (2005) 174710.
[18] A. Majchrowski, T. Łukasiewicz, J. Kisielewski, M. Świrkowicz, I.V. Kityk, A.H. Reshak, Mater. Lett. 63 (2009) 1410.
[19] M.O. Ramirez, D. Jaque, L.E. Bausá, I.R. Martín, F. Lahoz, E. Cavalli, A. Speghini, M. Bettinelli, J. Appl. Phys. 97 (2005) 093510.
[20] J. Suda, T. Mori, H. Saito, O. Kamishima, T. Hattori, T. Sato, Phys. Rev. B 66 (2002) 174302.
[21] M.P. Hehlen, A. Kuditcher, S.C. Rand, S.R. Luthi, Phys. Rev. Lett. 82 (1999) 3050.
[22] F. Auzel, C.R. Acad. Sci. Paris 262 (1966) 1016.